Study of basicity impact on mold flux crystallization and radiative heat transfer in continuous casting

Wanlin WANG, Lejun ZHOU, Kezhuan GU and Fanjun MA
School of Metallurgical Science and Engineering, Central South University Changsha, 410083, China

Abstract: This paper first investigated the temperature time transformation (TTT) diagrams and continuous cooling transformation (CCT) diagrams of mold fluxes with different basicity by using single hot thermocouple technology (SHTT). Results showed that: with the increase of basicity, the incubation time of isothermal crystallization became shorter; the crystallization temperature was getting higher; and the critical cooling rate of continuous cooling crystallization became faster. The X-ray diffraction analysis suggested that calcium silicate ($CaO{\cdot}SiO_2$) was precipitated at the upper part of the TTT diagram and cuspidine ($Ca_4Si_2O_7F_2$) was formed at the lower part, when the basicity of mold fluxes was within 1.0-1.2. Kinetic study indicated that the increase of the basicity tended to enhance the mold flux crystallization, and the crystallization mechanism of cupsidine was changing from one-dimensional growth to three-dimensional growth with a constant number of nuclei, when the basicity of mold fluxes varied from 0.8 to 1.2.

By using an infrared radiation emitter, a radiative heat flux was applied to a copper mold covered with solid mold flux disk to simulate the heat transfer phenomena in continuous casting. The crystallization behaviors of mold fluxes with different basicity and their impact on the radiative heat transfer were investigated dynamically. The results suggested that the basicity tends to enhance mold flux crystallization, leading to the reduction of radiative heat transfer rate and improvement of interfacial thermal resistance.

Keywords: Mold flux, TTT and CCT, radiative heat transfer, crystallization, basicity

1. Introduction

Mold flux has been widely used in continuous casting for lubricating the strand, adsorbing inclusions, moderating mold heat transfer and insulating the molten steel free surface. The mold flux crystallization was regarded as one of the most important properties of mold flux, as it primarily controls the heat transfer and lubrication in the continuous casting mold [1, 2]. The crystallization behavior of mold flux has been studied intensively. Kashiwaya et al [3] first developed the single hot thermocouple technology (SHTT) and double hot thermocouple technology (DHTT) for in situ observation and measurement of crystallization of mold flux. Cramb et al [4] considered the effect of water vapor on mold slag crystallization through using double hot thermocouple technology (DHTT). Orrling et al [5] discovered that crystal morphology of mold flux was dependent on the degree of undercooling. Some other researchers investigated the effect of chemical compositions like F^- [6], Na_2O [7], Li_2O [8], Al_2O_3 [9], rare earth oxide [10], et al on the crystallization behavior of mold flux. However, the basicity of mold flux has been regarded as the most significant effect on the mold flux crystallization. The study of K. C. Mill et al' [11] showed that the addition of CaO caused a dramatic increase in the amount of crystalline phase formed. H. G. RYU et al [12] found that the increase of basicity

tended to improve the crystallization temperature and reduce the incubation time by using a Confocal Scanning Laser Microscopy (CSLM). Although these were some results regarding basicity and mold flux crystallization being studied, very few researches have been developed to systematically study the effect of basicity on mold flux crystallization, especially in the view of kinetics.

As the basicity strongly affects the mold flux crystallization, and the crystallization further introduces a significant heat transfer reduction through two mechanisms, i.e., reduction of radiative heat transfer and enlargement of interfacial thermal resistance; it becomes necessary to understand how the basicity affects the radiative heat transfer and interfacial thermal resistance in continuous casting. However, there is very few research has been conducted to specify this effect, due to the difficulty in determining an exact expression for the radiative heat flux in continuous casting.

In this article, a kinetic study of the effect of basicity on mold flux crystallization was first carried out by using Hot Thermocouple Technology. Then, an infrared heat emitter was used to irradiate the surface of a copper mold that was covered with solid glassy mold flux disks with various basicities. Then the responding in-mold heat flux could be analyzed by the response of the subsurface mold temperatures. The experiments were also recorded by a digital camcorder to investigate the crystallization behavior of mold fluxes. Finally, the effect of basicity on the radiative heat transfer and interfacial thermal resistance was studied by analyzing the measured heat fluxes and the recorded images.

2. Experimental Method and Apparatus

2.1 TTT and CCT Tests of Mold Fluxes

The TTT and CCT tests of mold flux were conducted by using a single hot thermocouple technology. The details of SHTT/DHTT have been described by Kashiwaya [3], as shown in Figure 1.

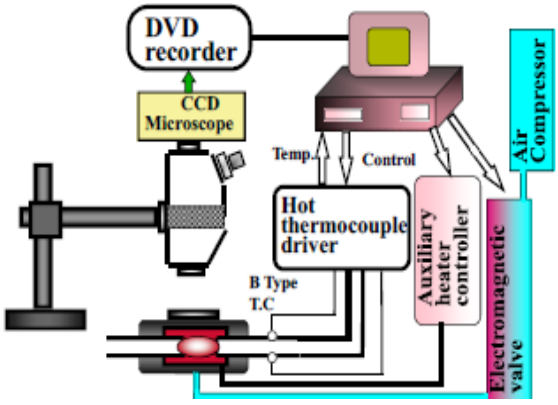

Fig. 1 the schematic of experimental apparatus [3]

Figure 2 showed a typical image of in situ observation of mold flux crystallization process by SHTT. A slag sample was mounted on a B type thermocouple which was heated directly while its temperature was recorded simultaneously. The crystal precipitated in the molten slag and was recorded by CCD for the observation and analysis. Thus, the crystallization process of various isothermal and non-isothermal could be studied.

The mold flux used in this study was an industrial low carbon steel mold flux with the basicity ($R=CaO/SiO_2$) of

0.8 as the matrix flux (Table I), then different amounts of CaO, Al_2O_3, MgO, CaF_2, Na_2O, Li_2O were added to make the basicity change from 0.8 to 1.2 and balance other components. The mixture was melted in an induction furnace at 1500°C for 5 minutes to homogenize its chemical composition, after that, it was poured into a cool steel plate to quench, and then it was subjected to crushing and grinding to make sample powders for the SHTT tests.

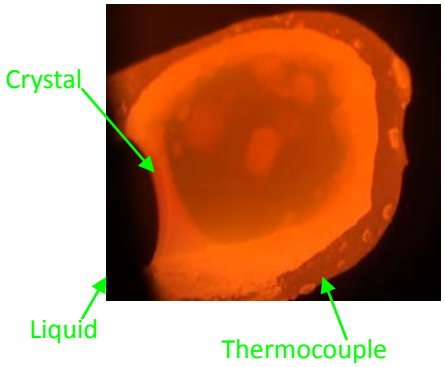

Fig. 2 In situ observation of mold flux crystallization process by SHTT

Table I. The Chemical Compositions of Pre-melted Mold Fluxes (in Mass Pct)

	CaO	SiO_2	Al_2O_3	MgO	F	Na_2O	Li_2O	Basicity
Flux1	33.53	42.03	6.81	2.07	5.84	9.18	0.54	0.8
Flux2	37.75	37.82	6.95	1.86	6.08	9.06	0.48	1.0
Flux3	39.55	35.98	7.11	1.94	5.93	8.98	0.51	1.1
Flux4	41.14	34.32	7.08	2.10	5.79	9.12	0.45	1.2

For the test of TTT, the thermocouple together with the powder sample was first heated to 1500°C at the rate of 15°C /s, and then, it was held for 5 min to eliminate bubbles and homogenize chemical composition. After that, it was rapidly cooled down to different temperatures for isothermal crystallization. For CCT tests, the sample was also heated to 1500 °C at the rate of 15 °C /s and held for 5 min, and then it was continuous cooled at different rates. The TTT and CCT diagrams were constructed by recording the relationship between the temperature, time and transformation.

In order to identify the phase composition of crystal mold flux at different noses area of TTT diagram, the X-ray diffraction was used.

2.2 Kinetic Study of Crystallization Process

The kinetics of mold flux isothermal crystallization involving nucleation and growth was analyzed through Johnson-Mehl-Avrami (JMA) model [13, 14]. According to the JMA model, the volume fraction of crystals (X) was given by:

$$X = 1 - \exp\{-[k(t-\tau)]^n\} \qquad (1)$$

Where t is crystallization time, τ is incubation time, k is the effective crystallization rate constant (including nucleation and growth), and n stands for Avrami exponent that is associated with the nucleation and growth mechanism.

The volume fraction of crystallization (X) obtained at a certain temperature was defined as, $X = A_c / A_T$, where A_C is the area of crystal and A_T is the total area of mold flux. The values of A_C and A_T were obtained by image analysis. The deviations can be controlled under ±0.025.

Therefore, the values of n and k could be determined according to the following equation by rearranging equation (1) into equation (2).

$$\ln\ln(\frac{1}{1-X}) = n\ln k + n\ln(t-\tau) \qquad (2)$$

By plotting lnln(1-X) versus ln(t-τ), the values of k and n could be obtained as the interception and slope of the regression line.

The effective crystallization rate constant (k) which was related to temperature T could also be determined via the Arrhenius Equation [15, 16]:

$$k = A\exp(\frac{-E_a}{RT}) \qquad (3)$$

Where, E_a is the activation energy of crystallization, A stands for the pre-exponential factor, R is the gas constant, and T means absolute temperature (notice the unit is K).

By rearranging equation (3), the value of E_a could also be determined by plotting lnk versus 1/(RT) from equation (4).

$$\ln k = \ln A - \frac{E_a}{RT} \qquad (4)$$

Therefore, the effect of basicity on mold flux crystallization could be analyzed through above kinetic study.

2.3 Heat Transfer Simulator

A schematic of the experimental apparatus was shown in Figure 3, the details of which have been described elsewhere. [17] The experimental apparatus mainly included: a power controller, an infrared radiant heater capable of emitting 2.0 MW/m^2 heat flux at the rate of 380 voltages, a data acquisition system and a command-and-control unit.

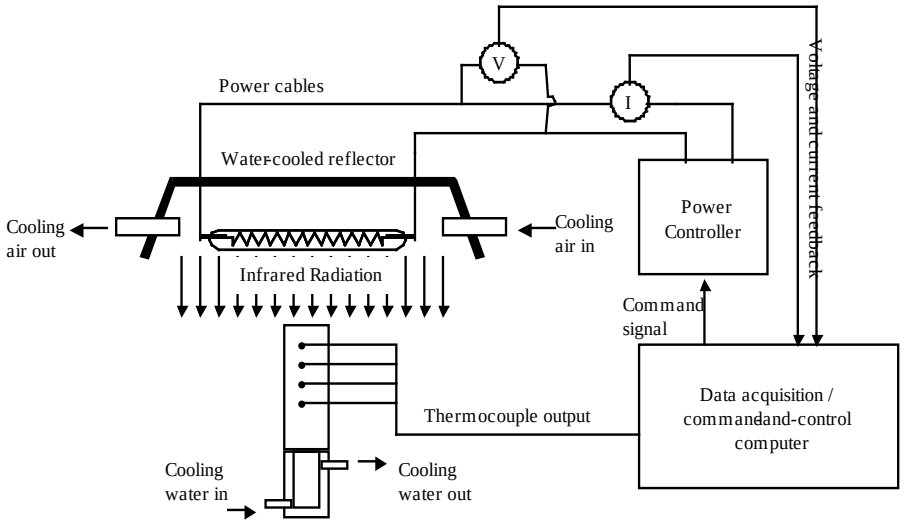

Fig. 3 Schematic illustration of the infrared emitter.

The copper mold was simulated by a one-end water cooled copper cylinder, which acted as the radiation target. As the heat flux was applied to the top surface of the copper mold, which was covered with mold flux disk, the response temperatures could be measured by the sub-surface thermocouples.

3. Results and Discussions

3.1 The TTT and CCT Diagrams of Mold Fluxes with Different Basicity

The TTT diagrams of mold fluxes with different basicity were shown in Figure 4. In the experiment, the 5 vol% of crystallization was defined as the beginning of crystallization, and the 95 vol% of crystallization was defined as the end of crystallization [18].

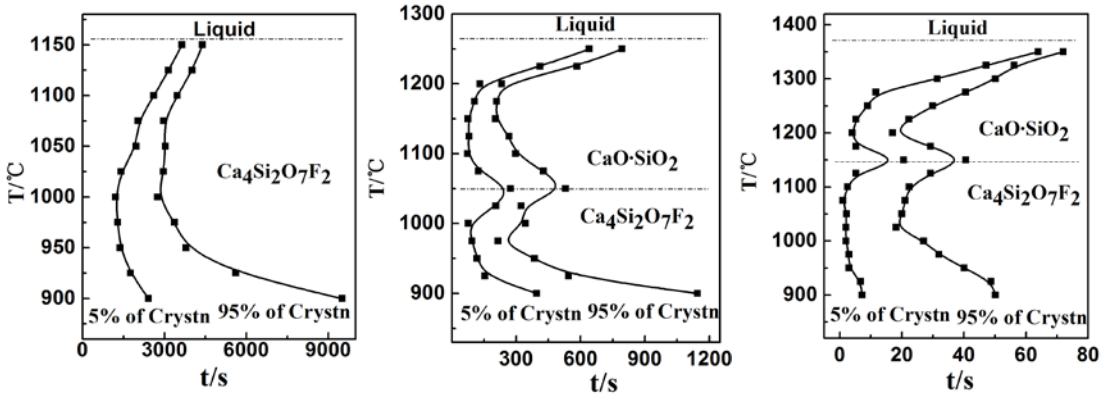

(a) R=0.8 (b) R=1.0 (c) R=1.1

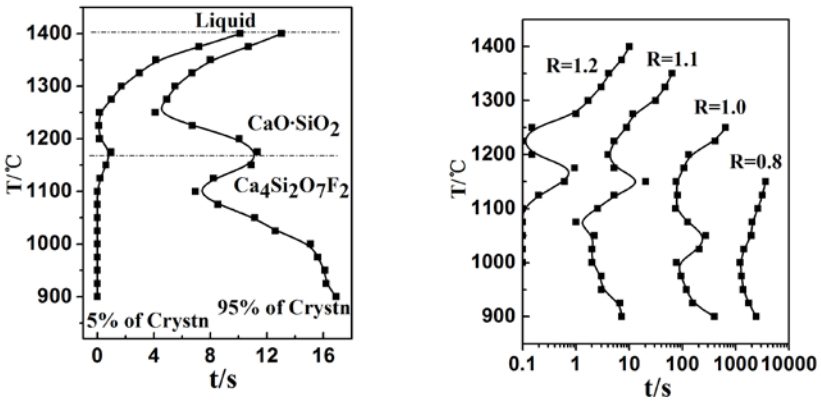

(d) R=1.2 (e) 5% of crystallization of R=0.8-1.2

Fig.4 TTT diagrams of mold fluxes with different basicity

It could be observed from Figure 4 (a) to (d) that all the curves were double noses except the R=0.8. This indicated that there were two separate crystallization processes occurred at the low and high temperature zone individually, when the basicity of mold fluxes was larger than 0.8. The phase composition of crystals was further identified by X-ray diffraction (Figure 5), and results showed that the crystal phase of R=0.8 and R=1.0-1.2 at lower temperature zone was cuspidine ($Ca_4Si_2O_7F_2$). While, calcium silicate ($CaO{\cdot}SiO_2$) precipitated at higher temperature zone for R=1.0-1.2 series fluxes.

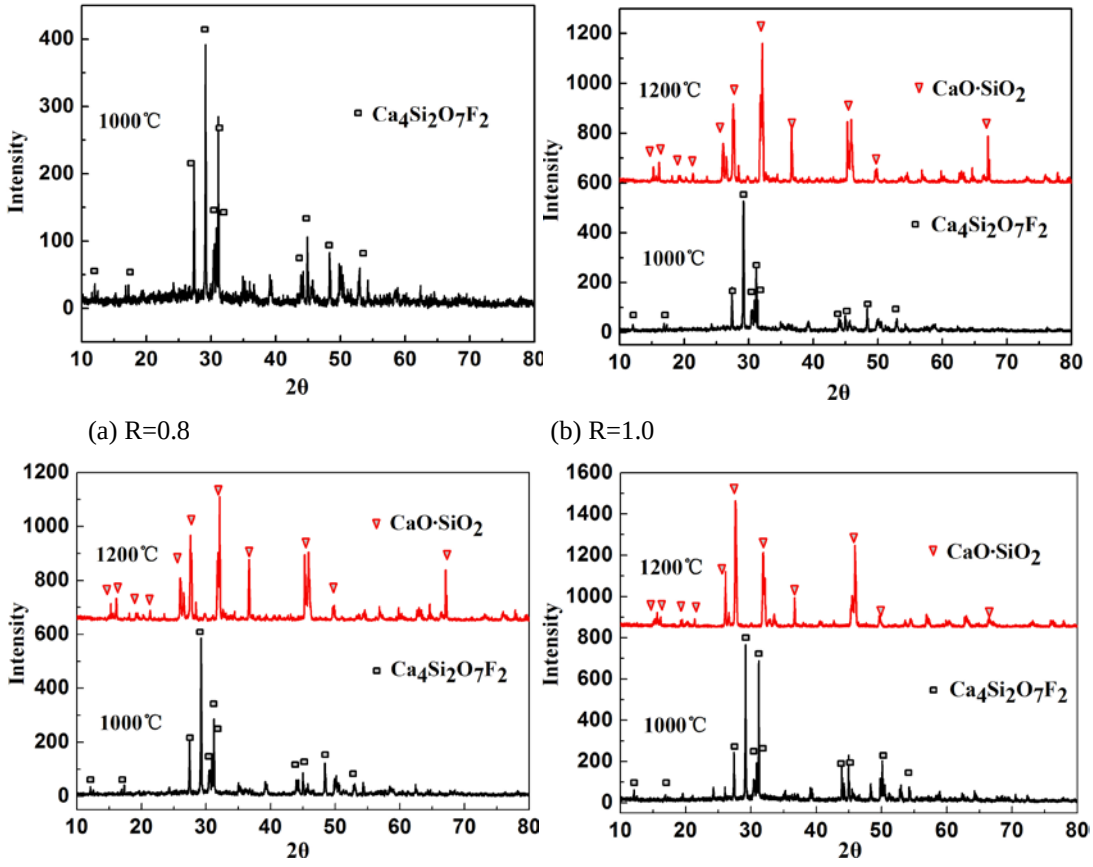

(a) R=0.8 (b) R=1.0

(c) R=1.1 (d) R=1.2

Fig.5 X-ray diffraction patterns of mold fluxes with different basicity

The incubation time was a very important parameter to characterize the crystallization property, and a shorter incubation time suggested an easier crystallization process. Figure 4 (e) combined all the four series 5 vol% of crystallization TTT curves and it suggested that the incubation time was getting shorter with the increase of mold flux basicity. For example, when the temperature held at 1000^0C, the incubation time for R=0.8 was about 1212 s. However, it was reduced to 77.4s, 2.0S and 0.1S, when basicity changed to 1.0, 1.1 and 1.2 respectively.

Figure 6 gave the CCT diagrams of the four series mold fluxes. It could be noticed that for the R=0.8 mold flux, the continuous cooling rates range was rather narrow, and the critical cooling rate was about 0.17°C/s, which indicated it was hard to form crystals during the operation of the industrial casting. However, when the basicity (NBO/T) value increased, the critical cooling rate was improved as shown in Fig 7 (a). The crystallization temperature was a strong function of both cooling rate and basicity. The increase of basicity tended to promote a higher crystallization temperature, and the crystallization temperature was increased from 956 to 1180, 1320 and 1402 °C as shown in Figure 7 (b), when the continuous cooling rate for four serials mold fluxes was kept at 0.17°C/s. The cooling rate would also dramatically influence the mold flux crystallization. For example, the mold flux, R=1.0, its crystallization temperature decreased from 1202°C to 963°C, when the cooling rate increased from 0.17°C /s to 12°C /s (Figure6 (b)). In figure 6(d), the crystallization temperature of mold flux R=1.2 was reduced linearly when the cooling rate changed from 20°C /s to 40°C /s. The reason may be due to the increase of molten slag viscosity with addition of cooling rate, and this required a larger driving force to initiate the crystallization. In other words, larger undercooling was needed [19].Therefore, the crystallization temperature decreased.

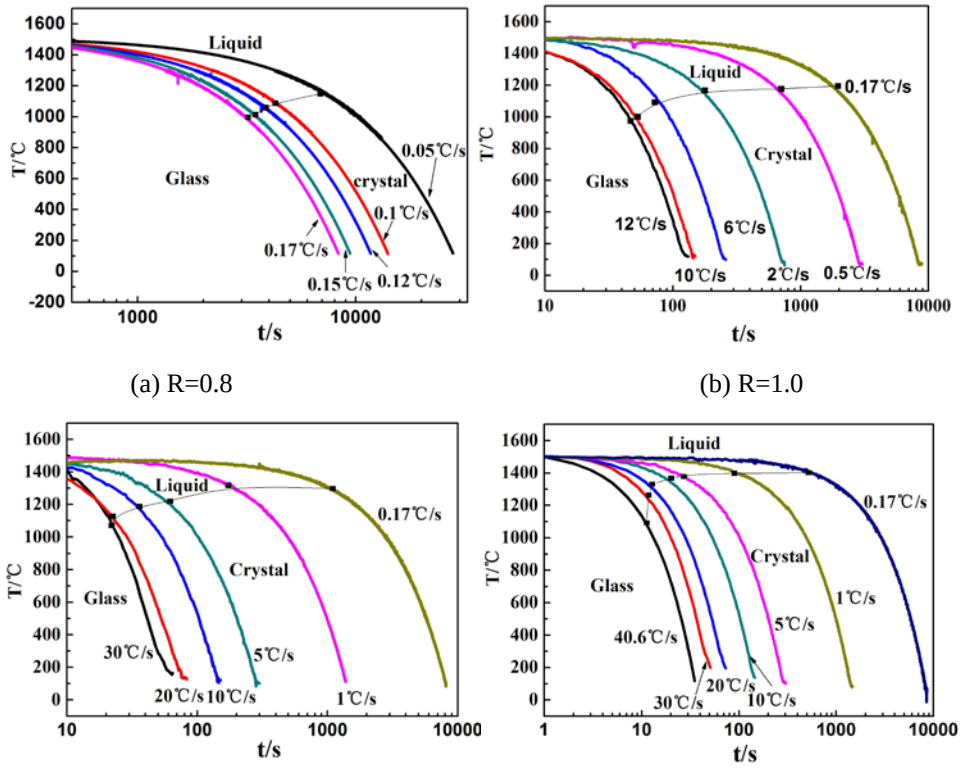

(a) R=0.8 (b) R=1.0

(c) R=1.1 (d) R=1.2

Fig. 6 CCT diagrams of mold fluxes with different basicity

The critical cooling rate versus basicity was plotted in Figure 7 (a). It indicated that: with the increase of mold flux basicity, the critical cooling rates increased. It changed from 0.17°C /s (R=0.8) to 12°C /s (R=1.0), 30°C /s (R=1.1) and 40.6°C /s (R=1.2). Thus, the glassy layer would be easily formed when the basicity was low and the crystals layer would appear when the basicity became high. Figure 7 (b) showed the crystallization temperature of mold fluxes versus basicity at the continuous cooling rate of 0.17°C /s. The crystallization temperature was linearly increasing from 956°C to 1402°C with the addition of basicity. This explained that why mold fluxes with high basicity was used in the casting of middle carbon steels or peritectic steels; while mold fluxes with low basicity was usually used in low carbon steels casting. Because, in the process of middle carbon steels or peritectic steels casting, mold fluxes with high crystallization temperature would reduce the heat flux in the mold to achieve a mild cooling of solidified shell. Therefore, the longitudinal cracking caused by uneven solidification can be reduced. On the contrary, due to the problem of breakout caused by sticking, low crystallization temperature mold fluxes were needed to keep the lubrication and enhance the heat transfer between mold and initial shell when the low carbon steels were casted [20, 21].

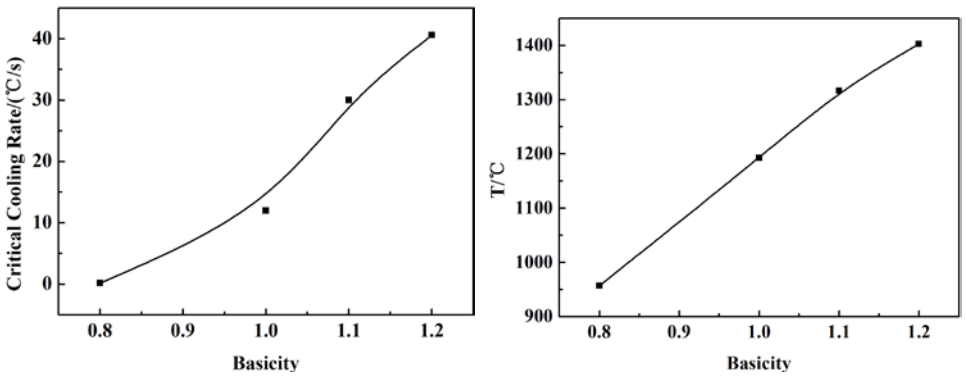

(a) (b)

Fig. 7 The critical cooling rates and crystallization temperature versus basicity

(a) The critical cooling rates of mold fluxes versus basicity; (b) Crystallization temperature of mold fluxes versus basicity at continuous cooling rate of 0.17℃/s

3.2 The Effect of Basicity on Effective Crystallization Rate and Crystallization Mechanism

Because cuspidine ($Ca_4Si_2O_7F_2$) was mainly formed in the lower part of the four series TTT diagrams, the isothermal crystallization processes at temperature ranging from 900°C -1050°C were chosen for the kinetic study. Plots of ln(ln(1/1-X)) versus ln(t-τ) for each individual mold flux crystallization was shown in Figure 8 (a)-(d), which gave the values of n as the slop of regression line and k as the interception as shown in equation (2) . The calculated values were listed in table II.

The variations of k in table II suggested the effective crystallization rate was increasing with the rise of hold temperature and mold flux basicity. These phenomena could be explained by the change of silicate structure and the transfer of ions in molten silicate system. High temperature environment was beneficial to the ions transfer, and the polymerization of silicate structures could be easy broken at high temperature. The same effect could be made by increasing the mold flux basicity. It was observed that the NBO/T of mold fluxes increased with the addition of basicity,

which indicated that the added O^{2-} provided by CaO can lower the degree of polymerization of silicate structures and decrease the viscosity of molten mold flux, which in turn would improve the effective crystallization rate [22].

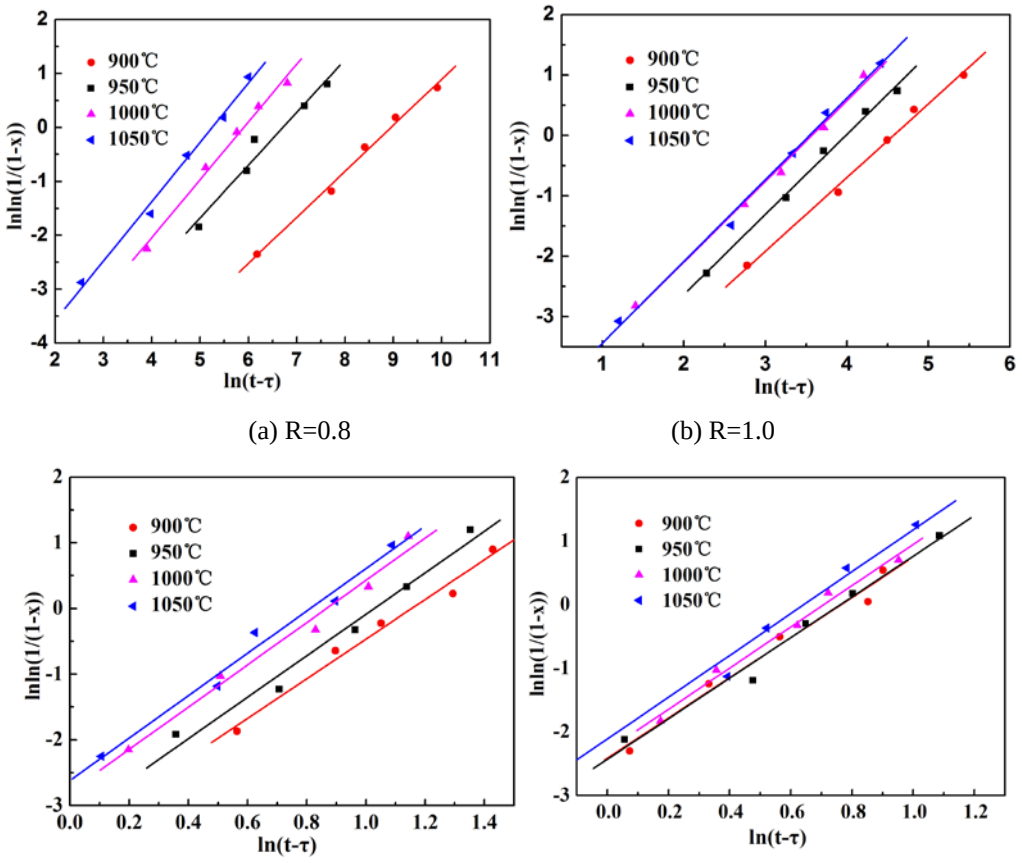

(a) R=0.8 (b) R=1.0

(c) R=1.1 (d) R=1.2

Fig. 8 The relation of crystal volume fraction evolution with function of time

According to JMA isothermal crystallization theory, different Avrami exponent n stands for different crystallization mechanism. J. W. Christian [23] has given out the corresponding relationship between n and the crystallization mechanism in his book in details. For the simplification, several researchers [22, 24] have summarized the general corresponding crystallization mechanism which listed in table III.

Table II: The variations of n and k versus basicity and temperature

Basicity (R)	Temperature	n	Lnk
0.8	900°C	0.85	-7.59
	950°C	0.98	-6.67
	1000°C	1.07	-6.31
	1050°C	1.1	-5.77
1.0	900°C	1.26	-5.75
	950°C	1.32	-5.26
	1000°C	1.33	-4.76
	1050°C	1.35	-4.73
1.1	900°C	3.02	-3.40

1.2	950°C	3.15	-3.26
	1000°C	3.2	-2.88
	1050°C	3.22	-2.54
	900°C	3.15	-2.48
	950°C	3.18	-2.43
	1000°C	3.24	-2.38
	1050°C	3.28	-2.24

Table III: Value of n for different nucleation and growth mechanism

	Crystallization Mechanism	
	Diffusion	Interface Reaction
Constant Nucleation Rate		
3-dimensional growth	2.5	4
2-dimensional growth	2	3
1-dimensional growth	1.5	2
Constant Number of Nuclei		
3-dimensional growth	1.5	3
2-dimensional growth	1	2
1-dimensional growth	0.5	1
Surface Nucleation	0.5	1

Compared with the values of n in table II and III, it was concluded that the growth mechanism of cuspidine crystal phase changed from low-dimension to high-dimension as the basicity increases in the temperature range from 900°C to 1050°C. When the basicity was 0.8, the n was about 1, indicating the cuspidine grew in the way of one-dimensional growth with a constant number of nuclei. However, when the basicity became 1.2, the n was around 3; thus, the cuspidine grew as three-dimensional growth.

3.3 The Variation of Crystallization Activation Energy

Figure 9 showed plots of lnk versus 1/RT for the four series of mold fluxes. The crystallization activation energy (Ea) was calculated from the slopes of the linear fits to the experimental data, as indicated in equation (4). The activation energy was computed as $E_{0.8}$=150.76±17.89kJ/mol, $E_{1.0}$=92.91±4.94kJ/mol, $E_{1.1}$=75.59±11.71kJ/mol and $E_{1.2}$=49.08±2.21kJ/mol individually. It implied that the crystallization activation energy decreased with the increase of mold fluxes basicity. These results may be also mainly associated with the basicity effects on viscosity and silicate structure, since the increase of O^{2-} concentration provided by CaO could simplify the silicate structure and decrease the viscosity of mold flux, which would reduce the transfer resistance of ion clusters and decrease the energy bar needed for the nucleation and growth of cuspidine.

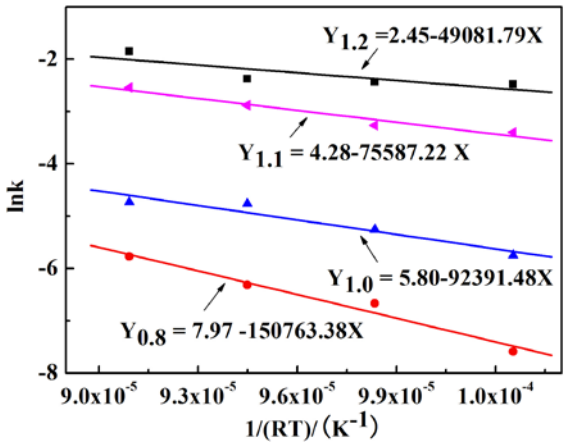

Fig. 9 Plots of lnk versus 1/RT for mold fluxes

3.4 The Effect of Basicity on Radiative Heat Transfer Rate

Four 3.3 mm thick glass disks with different basicity as shown in Table I were placed on the copper mold individually, and pre-heated by a 500 KW/m^2 thermal radiation. Then they were subjected to the constant thermal heating of 800 KW/m^2. The whole experiment process was recorded by digital camcorder to study the mold flux crystallization behavior.

The responding in-mold heat fluxes of R=0.8 were then calculated and shown in Figure 10. There were 4 stages appearing in the responding heat flux histories. Stage I: a period that the heat flux increases linearly with the addition of thermal radiation; stage II: the time from the deviation of the heat flux (due to the mold flux crystallization) to its peak value, where the incident energy came to constant; stage III: a attenuation stage where the heat flux continues to reduce under constant radiation due to the further crystallization; and stage IV: the period of steady state when the crystallization is completed and heat flux keeps constant. The images corresponding to each stage were also shown in Figure 10. From those pictures, it was clearly shown that these disks are fully glassy at stage I and then the opaque crystals are initiated at the top and developed toward the bottom due to the increasing of thermal radiation at stage II. With longer annealing time, a higher fraction of glassy disk is crystallized at stage III. Once the system steps into stage IV, there is no further crystallization, and the structure of disks are fixed; where the bottom of mold fluxes for R=0.8, 1.0 and 1.1 are keeping glassy, and the one for R=1.2 is completely crystallized (Figure 11).

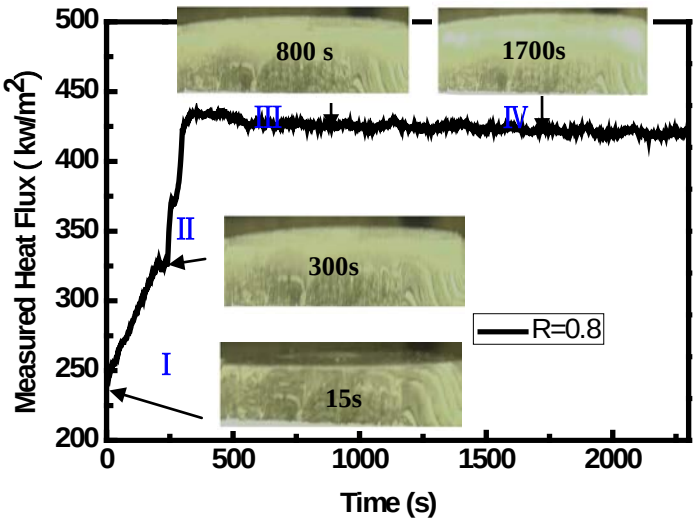

Fig. 10 The measured heat transfer rates for mold fluxes with R=0.8

In order to study the effect of basicity on the radiative heat transfer, the measured heat fluxes and the final cross-section views corresponding to each flux disk were given in Figure 11. It could be observed that the measured heat fluxes at steady state are around 423, 391, 378, 317 KW/m^2 for each individual disk. The steady state heat flux attenuates from 423 KW/m^2 to 317 KW/m^2 with the increase of the basicity. The thickness of crystalline layer and crystalline fraction for each disk were measured and shown in Figure12, where the thickness and crystalline fraction are 2.3mm and 69.8% respectively, when the basicity of slag is 0.8. While these two are changed to 3.3mm and 100%, as the basicity goes to 1.2. Therefore, it could be concluded that the basicity of mold flux does enhance the crystallization of mold flux, which lead to a further crystallization of mold fluxes when they were subjected to same thermal radiation. Consequently, the steady state heat flux rate decreased with the addition of mold flux basicity due to the increase of crystals fraction as shown in Figure 11, as there would be more incident radiation reflected and scattered from the crystals surface, grain boundary, and defects, such that there would be less energy absorbed and conducted to the mold.

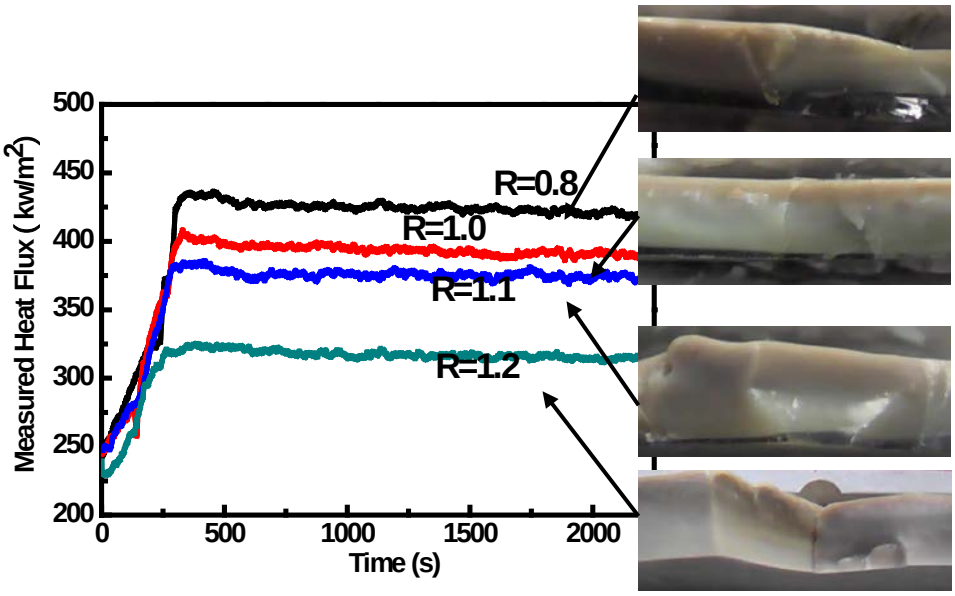

Fig. 11 The measured heat fluxes histories for different mold fluxes

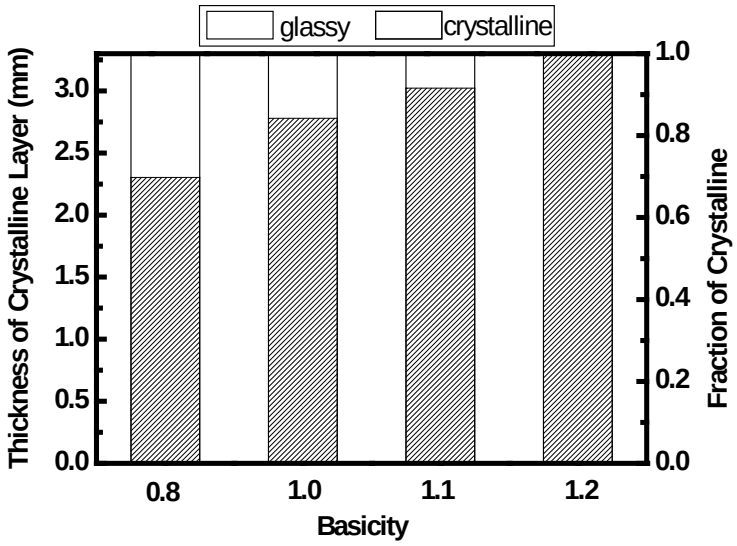

Fig. 12 Thickness of crystalline layer and the crystalline fraction of disks with different basicity

4. Conclusions

In the present paper, the crystallization kinetics of mold fluxes with different basicity was investigated by using a single hot thermocouple technology. The main conclusions were summarized as follows:

(1) The results of TTT tests showed that the TTT curves were double noses except the R=0.8 one. The X-ray diffraction analysis clarified that the crystal phase in higher temperature range was calcium silicate ($CaO{\cdot}SiO_2$) and cuspidine ($Ca_4Si_2O_7F_2$) in lower temperature range, when basicity was within 1.0-1.2. The incubation time of isothermal crystallization was getting shorter, with the increase of basicity.

(2) The results of CCT tests showed a higher basicity tended to improve the critical cooling rates and crystallization

temperature; and a higher cooling rate would reduce the crystallization temperature especially for the higher basicity mold fluxes.

(3) Kinetics study of isothermal crystallization process indicated that the effective crystallization rate constant k and Avrami exponent n became larger when temperature and basicity increased. The crystallization mechanism of cuspidine changed from one-dimensional growth to three-dimensional growth with a constant number of nuclei, when the basicity of mold fluxes increased from 0.8 to 1.2.

(4) The crystallization activation energy was calculated as: $E_{0.8}$=150.76±17.89kJ/mol, $E_{1.0}$=92.91±4.94 kJ/mol, $E_{1.1}$=75.59±11.71kJ/mol and $E_{1.2}$=49.08±2.21kJ/mol. This decreasing trend of E_a, together with the change of n and k, was mainly associated with the effects of basicity on the mold flux viscosity and silicate structure. The addition of the basicity increased the NBO/T of mold fluxes and simplified the silicate structure polymerization, resulted in viscosity decreasing and trend of crystallization increasing.

(5) Basicity enhances the mold flux crystallization, as the solid mold fluxes with a higher basicity would be further crystallized when they were subjected to same thermal radiation, and there would be a more thermal radiation scatted through the crystals boundary and defects, which resulted in a larger radiation reduction. The measured heat flux passing through the copper mold decreases with the increase of mold flux basicity. The steady state heat transfer rate changed from 413 KW/m^2 to 317 KW/m^2, when the basicity was increased from 0.8 to 1.2.

Acknowledgement

The work was supported by International Science & Technology Cooperation Program of China (2011DFA71390), New Century Excellent Talents Program Award (Chinese Ministry of Education, NCET-10-0797) and the Fundamental Research Funds for the Central Universities (2011JQ010).

References

[1] K. C. Mills, A. B. Fox, Z. Li and R. P. Thackray: *Ironmak Steelmak*, 2005, vol. 32 (1), pp. 26-34.

[2] Y. Meng, B. G. Thomas, A. A Polycarpou, H. Henein and A. Prasad: MS & T 2004 Conf. Proc., (New Orlean, LA), AIST, Warrendale, PA, 2004, pp. 57-67.

[3] Y. Kashiwaya, C. E. Cicutti, A. W. Cramb and K. Ishii: *ISIJ Int*, 1998, vol.38 (4), pp.348-356.

[4] C. Orrling and A. W. Cramb: *Metall. and Mater. Trans. B.*, 2000, vol. 31B, pp. 403-406.

[5] C. Orrling, S. Sridhar and A. W. Cramb: High temperature mater. proc., 2001, 20 (3-4): pp.195-200.

[6] T. Watanabe, H. Fukuyama, M. Susa and K. Nagata: *Metall. and Mater. Trans. B*, 2000, vol. 31B, pp. 1273-1281.

[7] M. Hanao, M. Kawamoto and T. Watanabe: *ISIJ Int*, 2004, vol.44 (5), pp.827-835.

[8] Y. Tan and D. Ju: *Mater. Sci. Forum*, 2011, vol.675-677, pp. 877-880.

[9] W. Wang, K. Blazek and A. W. Cramb: *Metall. and Mater. Trans. B*, 2008, vol.39B, pp. 66-74

[10] D. Wang, C. Liu, P. Shi, M and Jiang: *J. Iron Steel Res.*, 2004, vol. 16 (5), pp. 28-32.

[11] Z. Li, R. Thackray and K. C. Mills: VII Int. Conf. on Molten Slags, Fluxes and Slats, the South African Institute of Mining and Metallurgy, 2004, pp. 813-820

[12] H. G. Ryu, Z. T. Zhang, J. W. Cho, G. H. Wen and S. Sridhar. *ISIJ Int.*, 2010, vol.50 (8), pp.1142-1150.

[13] N. X. Sun, X. D. Liu and K. Lu: *Scripta Materialia*, 1996, vol. 34 (8), pp.1201-1207

[14] W. Wang: PhD thesis, Carnegie-Mellon University, 2007

[15] N. Boonyachut: PhD thesis, Carnegie-Mellon University, 2007
[16]A. A. Elabbar, M. Abu El-Oyoun and A. A. Abu-Sehly: JTUSCI, 2008, pp. 44-50.
[17] W. Wang and A. W. Cramb: *ISIJ Int*., 2005, vol. 45 (12), pp. 1864-70.
[18] Y. Kashiwaya, C. E. Cicutti and A. W. Cramb: ISIJ Int., 1998, vol. 38 (4), pp. 357-365.
[19] G. Wen, H. Liu and P. Tang: J. Iron Steel Res., Int., 2008, vol. 15 (4), pp.32-37.
[20] A. J Moore, R. J. Phillips and T. R. Gibbs: Steelmaking Conf. Proc., 1991, pp. 615-621.
[21] K. C. Mills, A. B. Fox, P. P. Thackray and Z. Li: VII International Conference on Molten Slags Fluxes and Salts, The South African Institute of Mining and Metallurgy, 2004, pp.713-721.
[22] K. Prapakorn: PhD thesis, Carnegie-Mellon University, 2003.
[23] J. W. Christian: The theory of transformations in metals and alloys. 3rd ed, Pergamon Press Ltd, London, 2002.
[24] D. R. MacFarlane and M. Fragoulis: *Phys. Chem. Glasses*, 1986, vol.37 (6), pp.228-234.